

# The Influence of Pluronic F68 and F127 Nanocarrier on Physicochemical Properties, *In vitro* Release, and Antiproliferative Activity of Thymoquinone Drug

Salwa Shaarani, Shahrul Sahul Hamid<sup>1</sup>, Noor Haida Mohd Kaus

Department of Physical Chemistry, School of Chemical Science, Universiti Sains Malaysia, <sup>1</sup>Oncological and Radiological Sciences Cluster, Advanced Medical and Dental Institute, Universiti Sains Malaysia, 13200 Bertam, Kepala Batas, Pulau Pinang, Malaysia

## ABSTRACT

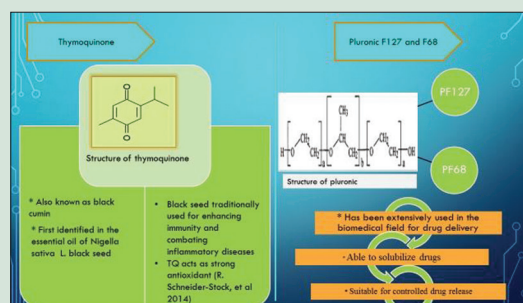
**Background:** This study reports on hydrophobic drug thymoquinone (TQ), an active compound found in the volatile oil of *Nigella sativa* that exhibits anticancer activities. Nanoformulation of this drug could potentially increase its bioavailability to specific target cells. **Objective:** The aim of this study was to formulate TQ into polymer micelle, Pluronic F127 (5.0 wt %) and Pluronic F68 (0.1 wt %), as a drug carrier to enhance its solubility and instability in aqueous media. **Materials and Methods:** Polymeric micelles encapsulated TQ were prepared by the microwave-assisted solvent evaporation technique. Fourier transform infrared spectroscopy and ultraviolet-visible spectrophotometer were utilized for qualitative confirmation of micelles encapsulation. The surface morphology and mean particle size of the prepared micelles were determined by using transmission electron microscopy (TEM). Cytotoxicity effect was studied using 3-(4,5-dimethylthiazol-2-yl)-5-(3-carboxymethoxyphenyl)-2-(4-sulfophenyl)-2H-tetrazolium, inner salt (MTS) assay. **Results:** Dynamic laser light scattering (DLS) technique showed hydrodynamic size distribution of optimized micelles of 50 nm, which was in close agreement with the mean particle size obtained from TEM of about 51 nm. Drug release study showed the maximum percentage of TQ release at 61% after 72 h, while the entrapment efficiency of TQ obtained was 46% using PF127. The cytotoxic effect of PF127-encapsulated TQ was considerably higher compared to PF68-encapsulated TQ against MCF7 cells, as they exhibited IC<sub>50</sub> value of 8 μM and 18 μM, respectively. **Conclusion:** This study suggests higher molecular weight Pluronic polymer micelles (F127) with hydrophilic-hydrophobic segments which could be used as a suitable candidate for sustainable delivery of TQ. However, comprehensive studies should be carried out to establish the suitability of Pluronic F127 as a carrier for other drugs with similar challenges as TQ.

**Key words:** Cytotoxicity, MCF-7 cell line, pluronic F68, thymoquinone-nanoparticle

## SUMMARY

There is a rising interest in integrating nanotechnology with medicine, creating a nanomedicine aiming for high efficiency and efficacy of disease diagnosis and treatment. In drug delivery, the term nanomedicine describes the nanometer-sized range (1-1000 nm) of a multi-component drug for disease treatments. As such, liposome-based nanoparticulate delivery vehicles have been approved by the Food and Drug Administration (FDA) for clinical applications. The main purpose of introducing nanoscale drug delivery is to improve the pharmacological and pharmacokinetic profiles of therapeutic molecules. Drug or therapeutic molecules can be either released through the cleavage of a covalent linkage between

drug molecules and polymers (conjugation) or through the diffusion from a drug and polymer blended matrix (physical encapsulation). Polymers play an important role in the design of nanocarriers for therapeutic deliveries. In Asia, *Nigella sativa* seed oil has been used traditionally for its various medicinal benefits. One of its most potent compound which is thymoquinone has been intensively investigated for its anti-cancer effects in colorectal carcinoma, breast adenocarcinoma, osteosarcoma, ovarian carcinoma, myeloblastic leukemia, and pancreatic carcinoma. In addition, it is reported to show anti-inflammatory potential, antidiabetic, antihistaminic effects, as well as the ability to alleviate respiratory diseases, rheumatoid arthritis, multiple sclerosis, and Parkinson's disease. This study aims to formulate and characterize different pluronic-based thymoquinone nanocarrier and investigate its effect against breast cancer cells.



**Abbreviations Used:** ATR-IR: Attenuated Total Reflectance-Infrared Spectroscopy, CH<sub>3</sub>CN: Acetonitrile, DLS: Dynamic Light Scattering, MTS: [3-(4,5-dimethylthiazol-2-yl)-5-(3-carboxymethoxyphenyl)-2-(4-sulfophenyl)-2H-tetrazolium, NPs: Nanoparticles, PF127/TQ: Pluronic F127 encapsulated TQ, PF68/TQ: Pluronic F68 encapsulated TQ, PLGA: Poly-(D,L)lactide-co-glycolide, PVA: Poly-vinyl-alcohol, TQ: Thymoquinone, UV/VIS: Ultraviolet-visible spectrophotometry

## Correspondence:

Dr. Noor Haida Mohd Kaus,  
School of Chemical Sciences,  
Universiti Sains Malaysia,  
Pulau Pinang, Malaysia.  
E-mail: noorhaida@usm.my  
DOI: 10.4103/0974-8490.199774

Access this article online

Website: www.phcogres.com

Quick Response Code:



## INTRODUCTION

There is an increasing interest in integrating nanotechnology with medicine, toward formulating nanomedicine aimed at high efficiency and efficacy of disease diagnosis and treatment.<sup>[1]</sup> Nanomedicine describes the nanometer-sized range (1–1000 nm) of a multi-component drug for disease treatments. The liposome-based nanoparticulate delivery system vehicles have been approved by the Food and Drug Administration for clinical application.<sup>[2]</sup> The main purpose of introducing nanoscale

This is an open access article distributed under the terms of the Creative Commons Attribution-NonCommercial-ShareAlike 3.0 License, which allows others to remix, tweak, and build upon the work non-commercially, as long as the author is credited and the new creations are licensed under the identical terms.

For reprints contact: reprints@medknow.com

Cite this article as: Shaarani S, Hamid SS, Mohd Kaus NH. The Influence of pluronic F68 and F127 nanocarrier on physicochemical properties, *in vitro* release, and antiproliferative activity of thymoquinone drug. Phcog Res 2017;9:12-20.

drug delivery is to improve the pharmacological and pharmacokinetic profiles of therapeutic molecules. Drug or therapeutic molecules can be either released through the cleavage of a covalent linkage between drug molecules and polymers (conjugation) or through the diffusion from a drug and polymer-blended matrix (physical encapsulation).

Polymers play an important role in the design of nanodrugs for therapeutic deliveries. There exists various polymeric nanomedicine for drug delivery systems such as polymer-protein conjugate,<sup>[3]</sup> polymer-small molecule conjugate,<sup>[4]</sup> dendrimer,<sup>[5]</sup> polymeric vesicle,<sup>[6]</sup> polymeric nanosphere,<sup>[7]</sup> and polymeric micelle.<sup>[8]</sup> Previous studies have reported on the formation of a poly (glycerol-succinic acid) dendrimer, in which building blocks such as glycerol and succinic acid are the natural metabolites.<sup>[9]</sup> This dendrimer exhibited a successful encapsulation of camptothecin (CPT), which is an anticancer drug with low water solubility.<sup>[10]</sup> Moreover, the dendrimer system has been reported to increase the aqueous solubility of CPT by approximately one order of magnitude. Furthermore, *in vitro* studies revealed that dendrimer enhances both the uptake and retention of these compounds within cancer cells.<sup>[11]</sup> Apart from that, polymer small molecule conjugate exhibited good track records since some preclinical success of these nanomedicine include *N*-(2-hydroxypropyl) methacrylamide copolymer, poly (glutamic acid) (PEG), (pGlu), dextran, and cyclodextrin-based polymer.<sup>[12]</sup> In addition, polymeric vesicle composed of polybutadiene is a well-known bilayer-forming polymer that can be subsequently cross-linked for enhanced vesicle stability.<sup>[13]</sup>

*N. sativa* seed oil is reported to have various medical benefits. It contains fixed oils, volatile oil, proteins, alkaloids, coumarins, saponins, minerals, carbohydrates, fiber, and water.<sup>[14]</sup> The plant has been reported to be commonly found in countries bordering the Mediterranean sea, Pakistan, and India.<sup>[15]</sup> It is reported that thymoquinone (TQ) inhibited the proliferation of several tumor cells such as colorectal carcinoma, breast adenocarcinoma, osteosarcoma, ovarian carcinoma, myeloblastic leukemia, pancreatic carcinoma, and brain tumor.<sup>[16,17]</sup> Moreover, TQ, the main active constituent of black seed oil, exhibits anti-inflammatory potential, antidiabetic and antihistaminic effects, as well as the ability to alleviate respiratory diseases, rheumatoid arthritis, multiple sclerosis, and Parkinson's disease.<sup>[18]</sup> Besides that, the antioxidant effect possessed by TQ has protected several organs against oxidative damage induced by free radical-generating agents such as doxorubicin-induced cardiotoxicity. Singh *et al.* reported that nanodrug-based formulation of TQ improves oral delivery stability assessment based on the *in vitro* and *in vivo* studies.<sup>[19]</sup> Despite having promising pharmaceutical activities, especially the anticancer properties, TQ suffers from severe bioavailability issue due to its hydrophobicity, hence poor solubility and instability in aqueous medium.<sup>[20]</sup> Recently, the development of polymeric nanomedicine has been studied on TQ with different methods used. Previous reports on TQ-loaded nanostructured lipid carriers were prepared by high-pressure homogenization technique and resulted in average particle size of  $75 \pm 2.4$  nm.<sup>[21]</sup> Moreover, another approach showed that TQ was employed in biodegradable nanoparticulate formulation based on poly (lactide-co-glycolide) (PLGA) and the stabilizer polyethylene glycol (PEG)-5000.<sup>[22]</sup> The other form includes TQ-encapsulated chitosan nanoparticles (CS NPs) which was used as drug delivery for nose-to-brain targeting.<sup>[23]</sup> Besides, TQ was reported to be successfully synthesized into 1,2-dipalmitoyl-*sn*-glycero-3-phosphocholine liposomal system, which was modified with Triton X-100 (XLP) by a conventional thin film hydration technique.<sup>[20]</sup>

To increase its stability and solubility in aqueous medium and hence its bioavailability, our study focused on two different Pluronic. The F127 and F68 (with PEO<sub>x</sub>/PPO<sub>y</sub>/PEO<sub>x</sub> molecular ratios of 99:67:99 and

76:30:76, respectively) were used for encapsulation of TQ into micelles in aqueous nanodispersion. The effectiveness of polymeric micelles depends on several factors such as the presence of different amphiphilic segments of copolymer which can influence the efficiency, stability, solubility, and *in vitro* release of the hydrophobic drug.

The use of Pluronic F127- and F68-encapsulated TQ has never been reported. Hence, in this study, the influence of two different polymeric micelles of Pluronic F127- and F68-encapsulated TQ was evaluated toward the physicochemical properties, *in vitro* release, and antiproliferative effect.

## MATERIALS AND METHODS

### Reagents

TQ (Sigma Aldrich, 99% purity), Pluronic F127 (molecular weight of 12,500 Da), and Pluronic F68 (molecular weight of 8500 Da) were purchased from Sigma-Aldrich. Acetonitrile is of analytical grade, and it was purchased from Fisher scientific. Mili-Q grade water was used for the preparation of all solutions. The established human breast cancer cell line MCF-7 was obtained from American Type Culture Collection. Phosphate-buffered solution was purchased from Fisher scientific and it was sterilized before use.

### Preparation of PF127- and PF68-encapsulated thymoquinone in aqueous phase

Initial step involved preparation of stock solution by dissolving in dimethyl sulfoxide. Followed by preparation of different concentrations comprising 0.3, 0.7, and 1.1 mM and dissolved in 1 ml acetonitrile. The emulsion formed was then stirred for 20 min. The PF127 and PF68 were dissolved in mili Q and then 20 ml of PF127 or PF68 was added. The colloidal suspension was then left to stir for overnight. It was then placed in a microwave (700 Watt) to evaporate the organic solvent. The study also utilized copolymer PF68 to encapsulate TQ to compare the differences with PF127. Finally, the suspension was filtered with a 0.22  $\mu$ m (biofilm) syringe filter to remove contaminants.

### Fourier transform infrared spectroscopic study

The PF127- and PF68-encapsulated TQ were examined by Attenuated Total Reflectance-Infrared (ATR-IR) spectrometer Frontier Perkin Elmer to confirm the success of encapsulation. The range of the scan covered from 4000 to 650  $\text{cm}^{-1}$ .

### Qualitative ultraviolet-visible spectrophotometric analysis

The synthesis of PF127 and PF68 encapsulated TQ was monitored by ultraviolet-visible (UV-VIS) spectrophotometer Shimadzu (UV 2600) to determine the maximum wavelength ( $\lambda_{\text{max}}$ ) of TQ, and the samples were scanned between 200 and 400 nm.

### *In vitro* drug release from pluronic formulation

The formulation of TQ loaded in two different systems, each PF127 and PF68, respectively, were placed in a dialysis bag (10 kDa MWCO, Thermo Scientific Inc., Rockford, IL, USA), suspended in 200 mL phosphate-buffered saline (PBS) at a pH of 7.4. To mimic the physiological condition of body systems, the samples were monitored at a constant temperature (37°C) while continuously stirring at 200 rpm. After each time interval, 3 mL of the samples was withdrawn and replaced with the same amount of fresh release medium. For each group, three samples were taken ( $n = 3$ ) for measurements. The amount of TQ released was determined by UV-VIS spectrophotometer.

## Determination of entrapment efficiency

Percentage of drug entrapped was evaluated in terms of the entrapment efficiency (% EE) with respect to the overall drug loaded in the formulation.

To determine the entrapment efficiency (% EE) of PF127- and PF68-encapsulated TQ, the samples were first sonicated for 3 min and vortexed for a few seconds. Drugs were then separated by ultracentrifugation at 14,000 rpm at room temperature for 30 min.

The resulting supernatant was collected and quantified spectrophotometrically (UV-VIS spectrophotometer Shimadzu) at 257 nm. The amount of drug entrapped (% EE) was calculated by the following equation:

$$\text{Percentage of EE} = \frac{\text{Amount of TQ in NPs}}{\text{Total amount of TQ}} \times 100\%$$

EE—entrapment efficiency

NPs-nanoparticle

## Cell culture and proliferation assay

The cells were cultured in RPMI-1640 (Gibco) media supplemented with 10% fetal bovine serum (JR Scientific) and antibiotics (10,000 Units/ml penicillin and 10,000 µg/ml streptomycin) (Gibco) under a humidified atmosphere containing 5% CO<sub>2</sub>. Each 96-well plate was seeded with a density of 3000 cells/well in 200 µl of fresh culture medium and incubated at 37°C under CO<sub>2</sub> atmospheric condition. The cells were then left to adhere to the plate before treatment with nanoparticles the concentrations of 0, 10, 20, 30, 40, 50, 60, 70, 80, 90, and 100 µM. Free TQ (without micelles), PF127-encapsulated TQ, and PF68-encapsulated TQ were treated for 24, 48, and 72 h, respectively. The medium was removed, and 100 µl of fresh medium mixed with 20 µl of CellTiter 96<sup>®</sup> AQ<sub>ueous</sub> nonradioactive cell (Promega, Madison, USA) proliferation assay was pipetted into each well. This reagent contained 3-(4,5-dimethylthiazol-2-yl)-5-(3-carboxymethoxyphenyl)-2-(4-sulfophenyl)-2H-tetrazolium (MTS) and phenazine methosulfate to quantify the number of viable cells in proliferation. Each well plate was incubated for 3 h at 37°C in a humidified condition of 5% CO<sub>2</sub> atmosphere.

Absorbance of each concentration was read at 490 nm using an ELISA microplate reader. The untreated cells were used as a negative control. Each concentration was repeated in quadruplicates. The amount of formazan product as measured at 490 nm absorbance is directly relative to the number of surviving cells in the samples. Percentage of cell viability was calculated as follows:

$$\text{Viability (\%)} = \frac{A_{\text{sample}}}{A_{\text{control}}} \times 100$$

## Statistical analysis

The experiments were done in quadruplicates, and the values were compared using one-way ANOVA performed in Statistical Package for the Social Sciences (SPSS) software IBM (Armonk, New York, USA).  $P < 0.05$  was considered statistically significant. All quantitative data were expressed as mean  $\pm$  standard deviation.

## RESULTS

### Attenuated Total Reflectance (ATR-IR)

The results of ATR-IP were depicted in Figure 1. Analysis indicated the presence of depression at similar wavenumber for raw TQ and TQ-nanoparticle in both pluronic PF68 and PF127.

### Ultraviolet-visible spectrophotometer

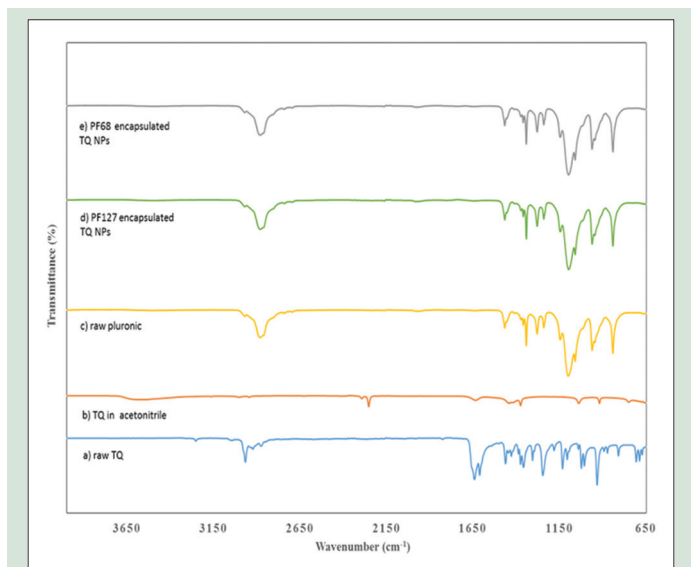
Analysis of nanoparticles using UV/VIS spectrophotometer showed peak absorbance at 257 nm with both pluronic and TQ acetonitrile as shown in Figures 2 and 3.

### Entrapment efficiency

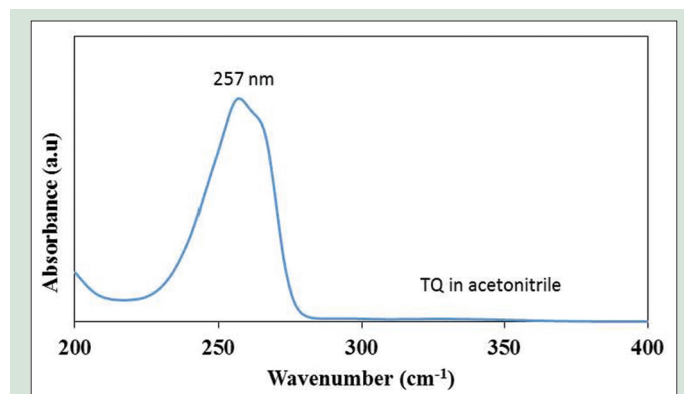
Percentage of weight per volume and entrapment efficiency measured in PF68 TQ-nanoparticle and PF127 TQ-nanoparticle were shown in Table 1. For PF68 TQ-nanoparticles, entrapment efficiency was highest with 0.1% weight per volume. It was noted that entrapment efficiency increased with increase in concentration. However, 5% weight per volume was selected.

### Transmission electron microscopy with thymoquinone loaded in 5% PF127

The TQ-nanoparticles were observed under transmission electron microscopy (TEM) to measure its size and morphology. Results provided in Figure 4 showed the difference in the sizes between 0.3 mM and 1.1 mM TQ. Regular-shaped particles formed with 1.1 mM TQ with an average size of 51 nm.



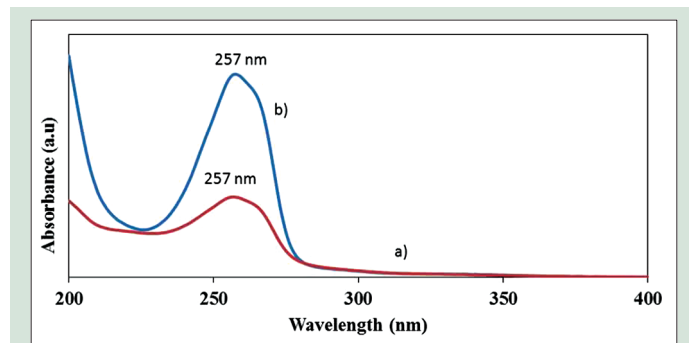
**Figure 1:** ATR-IR spectra of (a) raw thymoquinone, (b) thymoquinone in acetonitrile, (c) raw pluronic, (d) sample of lyophilized 5% PF127 encapsulated thymoquinone and (e) sample of lyophilized 0.1% PF68 encapsulated thymoquinone



**Figure 2:** Ultraviolet-visible spectrum showing maximum wavelength at 257 nm for control thymoquinone in acetonitrile

**Table 1:** Percentage for the amount of drug entrapped in the micelles core of each 1.1 mM of (a) PF68 encapsulated TQ and (b) PF127 encapsulated TQ. Data is presented as mean±standard deviation ( $n=3$ )

PF68 encapsulated TQ NPs		PF127 encapsulated TQ NPs	
Percentage of weight per volume (%)	Entrapment efficiency (%)	Percentage of weight per volume (%)	Entrapment efficiency (%)
0.1	42.1±1.21	5.0	46.6±1.03
0.5	35.4±1.09	7.5	49.2±0.85
1	33.9±2.75	10	60.1±0.55

**Figure 3:** Ultraviolet-visible spectrum showing maximum wavelength at 257 nm for 1.8 mM (a) PF68 encapsulated thymoquinone (b) PF127 encapsulated thymoquinone

### Transmission electron microscopy with thymoquinone loaded in 0.1% PF68

The TQ-nanoparticles were observed under TEM to measure its size and morphology. Results shown in Figure 5 indicate the difference in the sizes between 0.3 mM and 1.1 mM TQ. The 0.3 mM TQ produced particles with an average of 200 nm, but smaller particles were formed with 1.1 mM TQ with an average size of 40 nm.

### Transmission Electron Microscopy with PF127

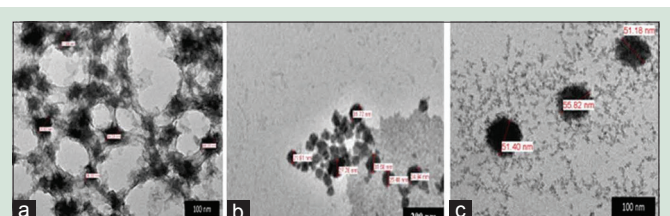
Based on an earlier finding, 1.8 mM was selected to formulate PF127 TQ-nanoparticles and size was determined using TEM as shown in Figure 6a. Hydrodynamic size showed an average of 50.75 nm and 7.53 nm [Figure 6b].

### Transmission electron microscopy with PF68

Further investigation with 1.1 mM PF68 TQ-nanoparticles showed sizes between 10 and 70 nm as shown in Figure 7a. However, hydrodynamic size showed peak at size of 41 nm [Figure 7b].

### Determination of zeta potential

The surface properties of nanoparticle drugs play a crucial factor because it affects the interaction with the local environment, which depends on a combination of size and surface properties. Furthermore, the surface properties will determine their solubility, stability, and clearance [41]. It was noted that the 0.3 mM polymeric micelles of PF127-encapsulated TQ exhibited the surface charge of  $-13.1 \pm 1.12$  mV, meanwhile the PF68-encapsulated TQ is  $-11.7 \pm 1.96$  mV. Surface charge of PF127/TQ and PF68/TQ formulated at a concentration of 0.7 mM exhibited zeta value of  $-4.29 \pm 0.79$  mV and  $-5.94 \pm 5.55$  mV, respectively. At highest molar concentration of 1.1 mM of both formulations, the zeta potential obtained increased to  $-15.3 \pm 0.36$  mV and  $-16.1 \pm 2.66$  mV, respectively.

**Figure 4:** Transmission electron microscopy images of PF127/thymoquinone at various concentration of (a) 0.3 mM, (b) 0.7 mM, and (c) 1.1 mM

### Drug release study

In the present study, maximum percentage of TQ released from the control system was 51%, meanwhile the release from encapsulated PF127 micelles was 62% in 48 h. The 1<sup>st</sup> h exhibited 44% of TQ released from control system [Figure 8a] whereas only 25% of TQ was released from the micelles system [Figure 8b]. The results revealed that TQ released from the polymeric micelle follows a slow and constant release rate compared to free TQ. It was noted that after 10 h the percentage of drug release was in a plateau.

Further experiment was carried out with 1.8 mM TQ-loaded 0.1% PF68, and the percentage of the drug release was 52% and similar to control [Figure 9a and b]. This was achieved within <10 h. It was also noted that further incubation did not show any increase in drug release. The 0.1% PF68 micelles showed complete drug release within 25 h.

### Effects of pH on the stability and solubility of thymoquinone-encapsulated PF127

The stability and solubility of TQ were evaluated by employing different pH values of gastrointestinal tract (pH 1, 5, and 7) in PBSs as well as in water dispersion. Tables 2 and 3 summarize the results of stability and solubility obtained from PF127- and PF68-encapsulated TQ, respectively. The solubility behavior for 3 consecutive days in various pH values showed almost similar solubility range from 51.40 to 72.67 µg/mL.

### Influence of storage time on the stability of PF127-encapsulated thymoquinone

The stability of formulated PF127 nanodrug is shown in Table 4. There were no significant changes in the physicochemical stability over storage period of 7, 14, and 21 days at room temperature.

### Dose- and time-dependent effects using cell viability assay

In this study, the cytotoxic effects of TQ NPs and TQ free were demonstrated on MCF-7 breast cancer cell lines based on time- and dose-dependent manner by using MTS assay. From the results in Figure 10, TQ NPs suppressed the growth of breast cancer cell lines

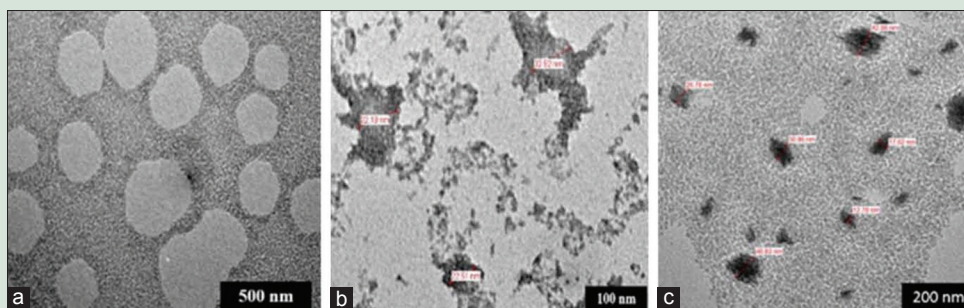


**Figure 5:** Transmission electron microscopy images of PF68/thymoquinone at various concentration of (a) 0.3 mM, (b) 0.7 mM, and (c) 1.1 mM

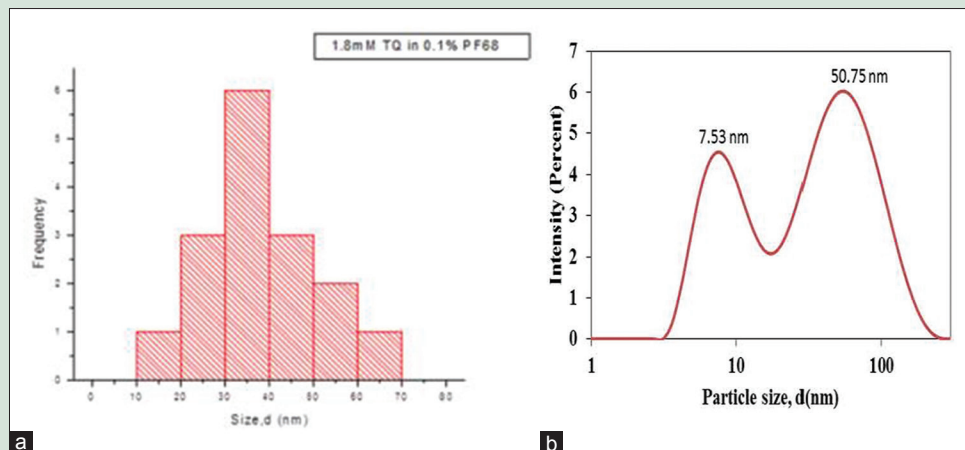


**Figure 6:** (a) Particle size distribution for polymer micelles 1.8 mm thymoquinone loaded 5% PF127 ( $70.93 \pm 17.55$ ) nm (b) average hydrodynamic size for polymer micelles 1.8 mm thymoquinone loaded 5% PF127

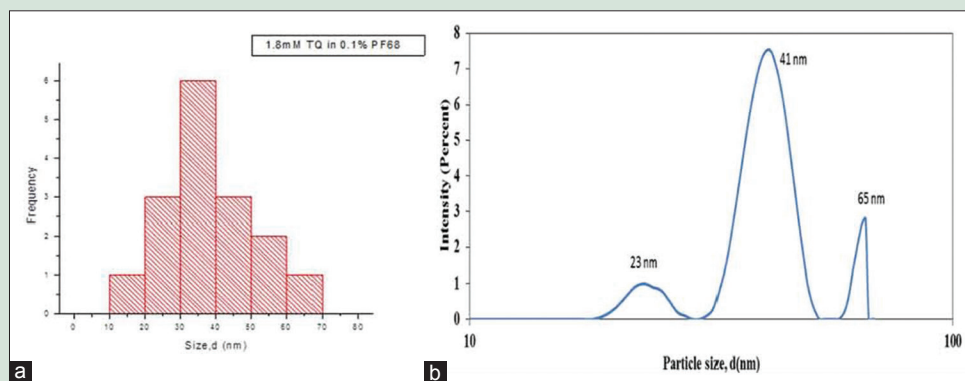


**Figure 7:** (a) Particle size distribution for 1.8 mM thymoquinone loaded 0.1% PF68 ( $37.74 \pm 12.94$ ) nm (b) Average hydrodynamic size for 1.8 mM thymoquinone loaded 0.1% PF68

**Table 2:** pH effects towards the stability and solubility of PF127/TQ

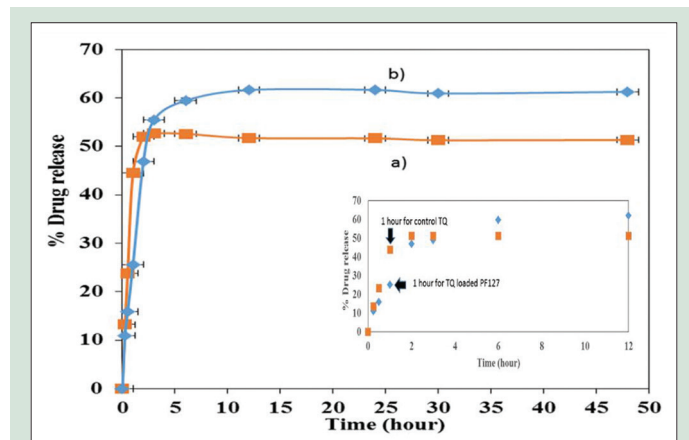
pH	Particle size (nm)	Zeta potential (mV)	Solubility( $\mu\text{g/mL}$ )		
			24 hours	48 hours	72 hours
1(PBS)	46	$0.04 \pm 0.75$	$85.05 \pm 0.02$	$95.94 \pm 0.01$	$81.66 \pm 0.02$
5(PBS)	30	$-6.76 \pm 1.03$	$98.98 \pm 0.01$	$98.99 \pm 0.01$	$91.54 \pm 0.01$
7(PBS)	30	$-6.73 \pm 0.58$	$103.24 \pm 0.03$	$80.58 \pm 0.03$	$92.08 \pm 0.02$
Water	50	$-15.3 \pm 0.36$	$67.92 \pm 0.06$	$41.49 \pm 0.01$	$33.26 \pm 0.00$

with  $IC_{50}$  values for TQ-loaded PF127 NPs after 24 h, 48 h, and 72 h determined at 20, 7, and 8  $\mu\text{M}$ , respectively. Meanwhile, TQ-loaded

PF68 NPs  $IC_{50}$  values after 24 h, 48 h, and 72 h were 30, 12, and 18  $\mu\text{M}$ , respectively [Figure 11].

**Table 3:** pH effects towards the stability and solubility of PF68/TQ

pH	Particle size (nm)	Zeta potential (mV)	Solubility( $\mu\text{g/mL}$ )		
			24 hours	48 hours	72 hours
1(PBS)	41	16.1 $\pm$ 1.25	61.81 $\pm$ 0.01	51.40 $\pm$ 0.00	63.28 $\pm$ 0.01
5(PBS)	53	-14.6 $\pm$ 0.21	69.14 $\pm$ 0.00	62.65 $\pm$ 0.01	53.53 $\pm$ 0.01
7(PBS)	59	-10.4 $\pm$ 0.95	72.67 $\pm$ 0.01	61.90 $\pm$ 0.01	55.04 $\pm$ 0.01
water	41	-16.1 $\pm$ 2.66	7.21 $\pm$ 0.00	6.79 $\pm$ 0.01	8.53 $\pm$ 0.00

**Figure 8:** Percentage drug release for control (a) thymoquinone in CH<sub>3</sub>CN and (b) PF127/thymoquinone micelles in 48 h

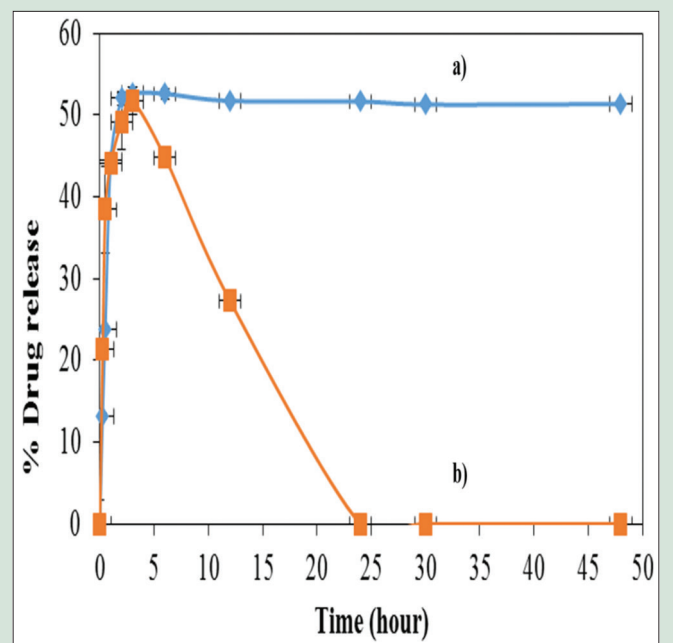
Antiproliferative effects of TQ free (without micelles) and the control were studied through morphological changes as shown in Figure 12. Images showed reduction in cell number and size over time when treated with PF68 and PF127 compared to the control pluronic.

## DISCUSSION

### Optimization of thymoquinone concentrations using Pluronic PF127 and PF68

This analysis was done to select the optimal concentration for TQ encapsulation with Pluronic P127 and P68. Three different concentrations of TQ were studied at 0.3 mM, 0.7 mM, and 1.1 mM in both Pluronic PF68 and PF127 formulations. At 0.3 mM PF127/TQ, the morphology was found to form a network of bridging interaction within the excess hydrophilic tail of polymeric micelles presence [Figure 1a]. At 0.7 mM, the morphology of the encapsulated nanodrug exhibited spherical shape with small aggregation of chain network [Figure 1b]. This shows better encapsulation of the polymer micelle F127 with good distribution and low aggregation. It is interesting to note that, at 1.1 mM, TQ-encapsulated PF127 showed a good spherical morphology and evenly distributed particles in the system [Figure 1c]. Next, the TQ formulation system using lower molecular weight polymer micelle of PF68 was studied. At lower concentration of 0.3 mM, TQ showed that there was no nanodrug formation based on the TEM images [Figure 2a]. This could be due to the encapsulation process using low-molecular weight of polymer micelles (PF68) with lower chain in core and corona which was not optimal for the entrapment of TQ. However, further increase in the concentration of TQ to 0.7 mM showed rough and indistinct shape of nanodrugs [Figure 5]. Increase in concentration up to 1.1 mM demonstrated that the TQ particles were encapsulated in more distinct shapes among the neighboring micelles as shown in Figure 5.

Based on these findings, it was noted that the formulation of TQ was dependent on drug concentration which affected the morphology and particle distribution of the encapsulated drug. It was noted that

**Figure 9:** Percentage drug release for (a) thymoquinone loaded in 0.1% PF68 and (b) control thymoquinone in CH<sub>3</sub>CN for 50 h, respectively

the 1.1 mM TQ to be optimal for encapsulation in both PF127 and PF68. It conclusively showed better encapsulation with discrete and homogeneous particles. Hence, this concentration was selected for further characterizations of physicochemical, *in vitro* release, and toxicity studies. Study on pluronic-based nanodrug stability based on particle size diameter, hydrodynamic size, and zeta potential. Particle size was measured using dynamic light scattering (DLS), and peak was noted with 1.1 mM PF127/TQ at 50.75 nm and another peak with smaller size of 7.65 nm. This represents excess free micelles in the dispersion. Analysis on similar concentration of TQ encapsulated with lower molecular weight of F68 showed peak at 41 nm with two distinct peaks at 23 nm and 68 nm. The three different peaks appeared due to the polydisperse nature of TQ nanodrug. It was noted that the particle size distribution of PF127/TQ and PF68/TQ was consistent with the TEM. Comparison with PF68/TQ showed its polydisperse distribution between 50 and 80 nm with an average size of 70.93  $\pm$  17.55 nm. It was higher in size compared to the PF127/TQ which had an average mean size of 37.74  $\pm$  12.94 nm.

Furthermore, our findings showed that lower absolute value of zeta potential was influenced by the nature of nonionic surfactants of Pluronic PF127 and PF68. The nanodrug particles were sterically stabilized by both polymer micelles, and the surface charges that are slightly negative is reported to assist in the cellular uptake and will minimize the nonspecific interaction toward cell membrane. As the value of surface charge increases (either negative or positive), macrophage scavenging will be increased and lead to greater clearance

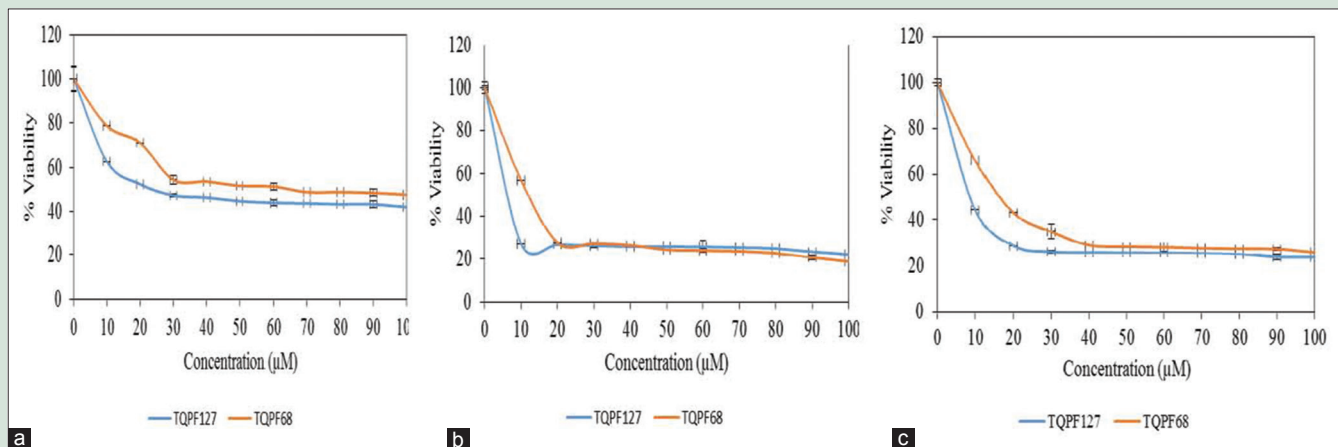


**Figure 10:** Difference in percentage of cell viability between PF127 and PF68 encapsulated thymoquinone NPs at (a) 24 hours treatment with thymoquinone nanocarrier, (b) 48 hours treatment with thymoquinone nanocarrier and (c) 72 hours treatment with thymoquinone nanocarrier

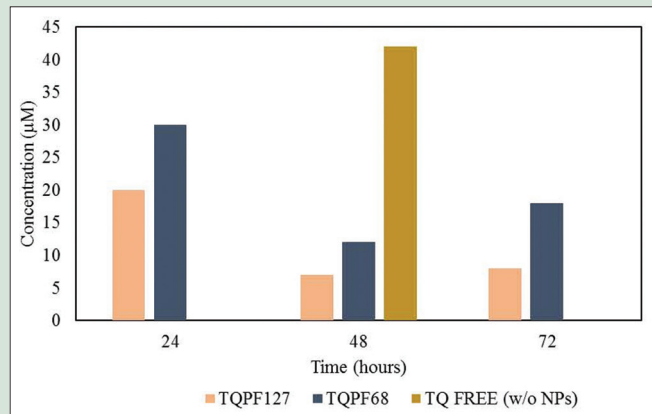


**Figure 11:** Half maximal inhibitory concentration (IC50) values for both pluronic formulations thymoquinone loaded PF127 and PF68 NPs

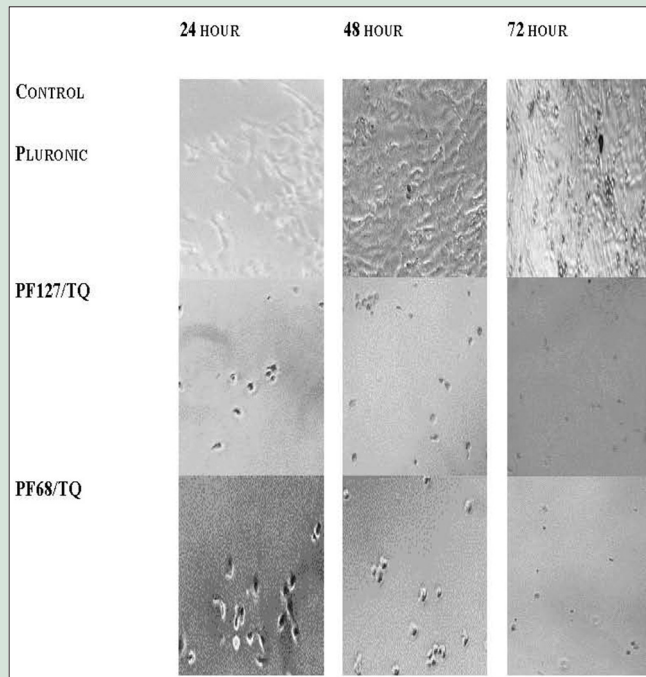


**Figure 12:** Morphological changes in MCF7 after treatment thymoquinone-nanodrug at different time point

**Table 4:** Particle size and zeta potential of thymoquinone-encapsulated PF127 after regular intervals of time

	Time (days)		
	7	14	21
Particle size (nm)	51	51	21
Zeta potential (mV)	-8.80±1.55	-9.98±4.42	-13.1±0.79

by the reticuloendothelial system, hence reduces the diffusion of nanodrugs to the target cells.<sup>[24]</sup>

### Effects of pH on the stability and solubility of thymoquinone-encapsulated PF127

The stability and solubility analyses showed that all encapsulated drugs sustained minimal degradation in phosphate buffer saline of pH 1 as particle size obtained was 46 nm. The size obtained is almost similar as in aqueous solutions. It can be concluded that the formulation is stable at extreme acidic condition. The solubility at 24 h, 48 h, and 72 h depicted a comparatively similar solubility ranging from 81.66 to 103.24 µg/mL for all examined pH values. However, specific solubility value is yet to be determined for TQ in these solutions due to the physical and chemical properties of the drug that may interfere with the soluble drug fraction.<sup>[25]</sup> Therefore, further reports are required to explore the possible

degradation pathways and the resultant products to have a better comprehensive study on the noted fluctuations in the solubility profile.

Findings on PF68-encapsulated TQ showed solubility characteristics for 3 consecutive days in various pH values that were almost similar with solubility range between 51.40 and 72.67 µg/mL. The fluctuations in characteristics might be due to volatile oil of TQ.<sup>[26]</sup> Nevertheless, the results suggested that TQ showed a good water solubility when incorporated in Pluronic aqueous solutions. It can be noted that utilizing lower molecular weight of Pluronic F68 with shorter chain of core and corona resulted in instability in the surface charge of the nanodispersion. At lower pH, zeta potential observed to be positively charged (16.1 ± 1.25 mV), and the values were decreasing as the pH of PBS increases.

Therefore, it can be concluded that the formulation of PF127/TQ nanodispersion exhibited better physicochemical properties compared

to the formulation of PF68/TQ. Figures 4 and 5 shows the correlation between the particle size and zeta values of PF127/TQ observed in different pH values. From the plot, PF127/TQ exhibited a low-negative zeta potential value and smaller particles size observed as the pH of the formulation in the buffer system increases. Previous works reviewed that the low-negative zeta potential would be useful in cellular uptake of TQ nanoparticles since it may assist in the reduction of electrostatic barrier which increases the chances of cellular uptake.<sup>[27]</sup> The buffer systems were used to mimic the physiological condition of gastrointestinal tract, and it is interesting to note that the results obtained confirmed that this nanodrug formulation was highly stable and soluble regardless of any pH dispersion, hence makes it useful in predicting the drug absorption throughout the gastrointestinal tract.

### Influence of storage time on the stability of thymoquinone-encapsulated PF127

This study indicated there were no significant changes on the physicochemical stability observed over a storage period of 7, 14, and 21 days at room temperature. The slight difference of zeta potential over storage time concluded that colloidal stability of nanodispersion was achieved due to steric repulsion that exists between polymers added into the system and was adsorbed onto the particle surface and thus prevent them from flocculating. If enough polymer adsorbs onto the particles, optimum thickness layer is achieved to keep particles separated by steric repulsions, and at this state, van der Waals interactions are too weak to adhere the particles together.<sup>[28]</sup>

The particle size of the nanodrug which maintained at 51 nm confirms that this formulation was stable up to 14 days and it is suitable for long-term administration. However, particle size was reduced to 21 nm after 21 days and might be due to the evaporation of TQ drug upon time.

### *In vitro* drug release

The maximum percentage of TQ released from the control system was 51%, whereas release from encapsulated PF127 micelles was 62% in 48 h. The 1<sup>st</sup> h exhibited 44% of TQ release from control system, however only 25% of TQ was released from the micelles system. The results revealed that TQ released from the polymeric micelle follow a slow and constant release rate compared to free TQ. Basically, in a micelle, there exists three different types of locations of drug, namely, the core, core–corona interface, and at the corona. In the core sections, the drug entrapped has the longest diffusional path relative to that of the drugs located at core–corona interface or known as hydrophobic–hydrophilic interface or the corona. The burst release is triggered by the drug located at the core–corona interface or corona.<sup>[29]</sup> In a control TQ system, a burst release pattern was based on the fact on the solubility of the drug and the partition coefficients which lead to rapid release due to thermodynamic imbalance.<sup>[30]</sup> On the contrary, Figure 8b depicted a slow TQ release profile which is due to the localization of drug at the core site after the encapsulation with PF127.

For drug release pattern of PF68-encapsulated TQ relative to the TQ in control CH<sub>3</sub>CN, findings at 1<sup>st</sup> h showed similar percentage of TQ release with 44%. The total maximum TQ release throughout the study for control TQ was 51%; however, for PF68 nanodrug formulation, it exhibited a gradual decrease after 3 h, and finally, there was no TQ release after 24 h. The results suggested that PF68 no longer can encapsulate TQ upon exposure to aqueous solution at longer time. This initial burst release pattern might be due to some amount of the drug was absorbed on the surface or loosely bound to the inner polymer core and was lost during the initial preparation stage. Apart from that, TQ is a volatile oil; hence, it has been evaporated toward the end of the study.

### Entrapment efficiency

The optimum entrapment efficiency for 5 wt% PF127- and 0.1 wt% PF68-encapsulated TQ was 46.6% and 42.1%, respectively. Theoretically, increase in the percentage of Pluronic F127 to more than 10% w/v would result in the formation of gel due to micellar enlargements. It is reported to be more entangled at higher concentration.<sup>[31]</sup> Furthermore, the number and size of micelles within the gel structure increase and cause a decrease in the number and dimension of water channels, consequently leading to higher viscosity and lower drug release rate. Therefore, even though PF127-encapsulated TQ showed highest percentage of TQ entrapped at 10% w/v of PF127, yet 5% w/v of PF127 was selected in this study.

### CONCLUSION

This study reports the differences in the characteristic of TQ-nanodrug formulated with pluronic F68 and F127. Encapsulation of TQ employing different molecular weights of amphiphilic triblock copolymer Pluronic F127 and Pluronic F68 in aqueous nanodispersion was performed by using emulsion-solvent evaporation technique. Characterization was done with ATR-IR, UV/VIS, TEM, and DLS analysis. The triblock copolymer assembled into spherically shaped structure with PEO hydrophilic chain at the hydrated segments and trapped TQ drug at the inner core of hydrophobic PPO in aqueous phase with smaller dimension of particle size. PF127/TQ and PF68/TQ were sterically stabilized with low-negative zeta potential values. PF127/TQ nanodispersion showed enhanced in solubility and stability regardless of any pH as to mimic the condition present in human gastrointestinal tract. A hydrophobic drug TQ was efficiently encapsulated in the core of Pluronic micelles. Higher entrapment efficiency was obtained from PF127-encapsulated TQ and more sustained release of drug relative to that of PF68-encapsulated TQ in aqueous nanodispersion. As compared to the PF68 nanodispersion, PF127 nanodispersion system exhibited higher toxicity toward MCF-7 cell lines. Stability of PF127 nanodispersion system was maintained up until 14 days duration of storage. Thus, different molecular weights and number of hydrophilic–hydrophobic segments of Pluronic showed significant results on the physicochemical properties, *in vitro* release, and antiproliferative effect of TQ drug toward MCF-7 cancer cell. It can be concluded that higher molecular weight with longer hydrophilic–hydrophobic segments of Pluronic polymer micelles (F127) could be used as a suitable candidate for the sustained delivery of drugs.

### Financial support and sponsorship

This study was funded by Universiti Sains Malaysia RUI grant 1001/CIPPT/812138.

### Conflicts of interest

There are no conflicts of interest.

### REFERENCES

- Arulkumar S, Sabesan M. Rapid preparation process of antiparkinsonian drug *Mucuna pruriens* silver nanoparticle by bioreduction and their characterization. *Pharmacognosy Res* 2010;2:233-6.
- Barenholz Y. Liposome application: Problems and prospects. *Curr Opin Colloid Interface Sci* 2001;6:66-77.
- Veronese FM, Pasut G. PEGylation, successful approach to drug delivery. *Drug Discov Today* 2005;10:1451-8.
- Chandran SS, Nan A, Rosen DM, Ghandehari H, Denmeade SR. A prostate-specific antigen activated N-(2-hydroxypropyl) methacrylamide copolymer prodrug as dual-targeted therapy for prostate cancer. *Mol Cancer Ther* 2007;6:2928-37.
- Gopin A, Ebner S, Attali B, Shabat D. Enzymatic activation of second-generation dendritic prodrugs: Conjugation of self-immolative dendrimers with poly (ethylene glycol) via click chemistry. *Bioconjug Chem* 2006;17:1432-40.

6. Lee JS, Feijen J. Polymersomes for drug delivery: Design, formation and characterization. *J Control Release* 2012;161:473-83.
7. Gref R, Minamitake Y, Peracchia MT, Trubetsky V, Torchilin V, Langer R. Biodegradable long-circulating polymeric nanospheres. *Science* 1994;263:1600-3.
8. Jhaveri AM, Torchilin VP. Multifunctional polymeric micelles for delivery of drugs and siRNA. *Front Pharmacol* 2014;5:77.
9. Degoricija L, Bansal PN, Söntjens SH, Joshi NS, Takahashi M, Snyder B, *et al.* Hydrogels for osteochondral repair based on photocrosslinkable carbamate dendrimers. *Biomacromolecules* 2008;9:2863-72.
10. Kong X, Yu K, Yu M, Feng Y, Wang J, Li M, *et al.* A novel multifunctional poly (amidoamine) dendrimeric delivery system with superior encapsulation capacity for targeted delivery of the chemotherapy drug 10-hydroxycamptothecin. *Int J Pharm* 2014;465:378-87.
11. Morgan MT, Nakanishi Y, Kroll DJ, Griset AP, Carnahan MA, Wathier M, *et al.* Dendrimer-encapsulated camptothecins: Increased solubility, cellular uptake, and cellular retention affords enhanced anticancer activity *in vitro*. *Cancer Res* 2006;66:11913-21.
12. Schluep T, Cheng J, Khin KT, Davis ME. Pharmacokinetics and biodistribution of the camptothecin-polymer conjugate IT-101 in rats and tumor-bearing mice. *Cancer Chemother Pharmacol* 2006;57:654-62.
13. Discher DE, Ahmed F. Polymersomes. *Annu Rev Biomed Eng* 2006;8:323-41.
14. Muhammad A, Randhawa S, Al-Ghamdi M. A review of the pharmacotherapeutic effects of *Nigella sativa*. *J Med Res* 2002;41:40-50.
15. El-Dakhakhny M, Barakat M, El-Halim MA, Aly SM. Effects of *Nigella sativa* oil on gastric secretion and ethanol induced ulcer in rats. *J Ethnopharmacol* 2000;72:299-304.
16. Ravindran J, Nair HB, Sung B, Prasad S, Tekmal RR, Aggarwal BB. Thymoquinone poly (lactide-co-glycolide) nanoparticles exhibit enhanced anti-proliferative, anti-inflammatory, and chemosensitization potential. *Biochem Pharmacol* 2010;79:1640-7.
17. Ashour AE, Ahmed AF, Kumar A, Zoheir KM, Aboul-Soud MA, Ahmad SF, *et al.* Thymoquinone inhibits growth of human medulloblastoma cells by inducing oxidative stress and caspase-dependent apoptosis while suppressing NF- $\kappa$ B signaling and IL-8 expression. *Mol Cell Biochem* 2016;416:141-55.
18. Schneider-Stock R, Fakhoury IH, Zaki AM, El-Baba CO, Gali-Muhtasib HU. Thymoquinone: Fifty years of success in the battle against cancer models. *Drug Discov Today* 2014;19:18-30.
19. Singh A, Ahmad I, Akhter S, Jain GK, Iqbal Z, Talegaonkar S, *et al.* Nanocarrier based formulation of Thymoquinone improves oral delivery: Stability assessment, *in vitro* and *in vivo* studies. *Colloids Surf B Biointerfaces* 2013;102:822-32.
20. Odeh F, Ismail SI, Abu-Dahab R, Mahmoud IS, Al Bawab A. Thymoquinone in liposomes: A study of loading efficiency and biological activity towards breast cancer. *Drug Deliv* 2012;19:371-7.
21. Abdelwahab SI, Sheikh BY, Taha MM, How CW, Abdullah R, Yagoub U, *et al.* Thymoquinone-loaded nanostructured lipid carriers: Preparation, gastroprotection, *in vitro* toxicity, and pharmacokinetic properties after extravascular administration. *Int J Nanomedicine* 2013;8:2163-72.
22. Shah M, Choi MH, Ullah N, Kim MO, Yoon SC. Synthesis and characterization of PHV-block-mPEG diblock copolymer and its formation of amphiphilic nanoparticles for drug delivery. *J Nanosci Nanotechnol* 2011;11:5702-10.
23. Alam S, Khan ZI, Mustafa G, Kumar M, Islam F, Bhatnagar A, *et al.* Development and evaluation of thymoquinone-encapsulated chitosan nanoparticles for nose-to-brain targeting: A pharmacoscintigraphic study. *Int J Nanomedicine* 2012;7:5705-18.
24. Davis ME, Chen ZG, Shin DM. Nanoparticle therapeutics: An emerging treatment modality for cancer. *Nat Rev Drug Discov* 2008;7:771-82.
25. Salmami JM, Asghar S, Lv H, Zhou J. Aqueous solubility and degradation kinetics of the phytochemical anticancer thymoquinone; probing the effects of solvents, pH and light. *Molecules* 2014;19:5925-39.
26. Gali-Muhtasib H, Roessner A, Schneider-Stock R. Thymoquinone: A promising anti-cancer drug from natural sources. *Int J Biochem Cell Biol* 2006;38:1249-53.
27. Bhattacharya S, Ahir M, Patra P, Mukherjee S, Ghosh S, Mazumdar M, *et al.* PEGylated-thymoquinone-nanoparticle mediated retardation of breast cancer cell migration by deregulation of cytoskeletal actin polymerization through miR-34a. *Biomaterials* 2015;51:91-107.
28. Zeta Potential: An Introduction in 30 Minutes. Available from: <http://www.malvern.com/en/support/resource-center/technical-notes/TN101104ZetaPotentialIntroduction.aspx>. [Last accessed on 2005 Apr 07].
29. Gill KK, Kaddoumi A, Nazzal S. PEG-lipid micelles as drug carriers: Physicochemical attributes, formulation principles and biological implication. *J Drug Target* 2015;23:222-31.
30. Huang X, Brazel CS. On the importance and mechanisms of burst release in matrix-controlled drug delivery systems. *J Control Release* 2001;73:121-36.
31. El-Kamel AH. *In vitro* and *in vivo* evaluation of Pluronic F127-based ocular delivery system for timolol maleate. *Int J Pharm* 2002 8;241:47-55.



Noor Haida Mohd Kaus

### ABOUT AUTHOR

Dr. Noor Haida Mohd Kaus is a senior lecturer at School of Chemical Sciences, Universiti Sains Malaysia.